

Optically realizable localized wave solutions of the homogeneous scalar wave equation

Kaido Reivelt and Peeter Saari

Institute of Physics, University of Tartu, Riia 142, 51014 Tartu, Estonia

(Received 19 December 2001; published 11 April 2002)

One of the most frequently discussed problems in construction of localized wave (LW) solutions of the homogeneous scalar wave equation has been their energy content—the LW's generally have infinite energy content and special methods have to be used to obtain physically realizable wave fields. So far the problem has mainly been addressed as a pure mathematical one and the proposed LW's can hardly be implemented in optics. In this paper we propose an approach for constructing physically realizable LW's that have a transparent interpretation in terms of optical setups. It will be shown that such LW's can be derived as finite aperture approximations of fundamental LW's, the focus wave modes.

DOI: 10.1103/PhysRevE.65.046622

PACS number(s): 42.25.Bs, 42.15.Eq, 42.65.Re, 41.20.Jb

I. INTRODUCTION

The free-space propagation of electromagnetic wave fields is generally known as one of the most thoroughly investigated processes in optics. However, in recent years renewed research interest in this field has arisen, as a novel class of ultrawideband transient solutions of homogeneous wave equation—so called localized waves (LW)—have been introduced and investigated extensively (see, e.g., Refs. [1–16], and references therein).

The reason for the interest is the peculiar propagation of those wave fields—the spatial amplitude distribution of LW's can be designed to consist of a micrometer diameter central peak on a sparse, low intensity background. From the viewpoint of diffraction theory, the transversal and longitudinal spread of such a pulse should be very substantial. However, in the theoretical limit the amplitude distribution of many LW's does not spread at all as it travels in free space [3,6].

Obviously, the optical implementation of such wave fields could be very attractive for the applications where the lateral and(or) transversal diffractive spread of the wave fields is a major limitation of the system performance (e.g., optical communication, metrology, monitoring, imaging, and femtosecond spectroscopy). However, the mathematical description of those ultrawideband, nontrivial wave fields have proved to be intricate and despite all the theoretical work done so far, there are still several topics that need to be clarified before the optical implementation could be successful.

One of the most important and widely discussed arguments that has cast serious doubts on the feasibility of LW's is the fact that the total energy content as well as the energy flow of the fundamental LW's—focus wave modes (FWM)—is infinite and thus they cannot be generated in a real optical setup (see Refs. [6–8], and references therein). The problem has been overcome mainly by constructing various finite energy flow approximations to the FWM's. For example, the problem has been addressed as a pure mathematical one: given the analytical expression of FWM's,

$$\begin{aligned} \Psi_{FWM}(\rho, z, t; a_1, \beta) \\ = \frac{1}{4\pi(a_1 + i\sigma)} \exp\left[-\frac{\beta\rho^2}{a_1 + i\sigma}\right] \exp[i\beta\tau], \quad (1) \end{aligned}$$

where $\rho = \sqrt{x^2 + y^2}$, $\sigma = z - ct$, $\tau = z + ct$, and a_1, β are parameters, the finite energy flow LW's have been constructed as the superpositions of the FWM's of the form [5–7]

$$\Psi_{LW}(\rho, z, t; \beta) = \int_0^\infty d\beta F(\beta) \Psi_{FWM}(\rho, z, t; a_1, \beta). \quad (2)$$

It has been shown [6,7], that by means of a careful choice of the weighting function $F(\beta)$ and the parameter a_1 , the superpositions (2) can be constructed so that the resulting wave field has both finite energy density and finite total energy. However, no interpretation in terms of optical setups has been given for those wave fields so far.

Also, several studies have introduced finite energy flow LW's by applying a finite-time dynamic aperture on an infinite energy LW pulse (see, e.g., Refs. [7–10], and references therein). But again, such an idea is difficult to realize in optical domain since its physical realization would require an electrically short and thin, center-fed, linear dipole antenna possessing a matrix of independent elements each excited by a specific broadband time-dependent signal [7].

In this paper we construct a class of LW's, that (1) have finite energy flow and (2) are realizable by means of a practical optical setup. After giving some introductory notes in Sec. II we use well-known properties of monochromatic Bessel beams to derive a mathematical expression for the LW's and propose an optical setup for their generation. In Secs. III and IV a numerical example and some experimental considerations will be presented.

II. FOURIER REPRESENTATION OF FUNDAMENTAL LW'S—FWM'S

In Fourier representation an axisymmetric scalar wave field in free space can be described as a superposition of monochromatic Bessel beams as

$$\begin{aligned} \Psi(\rho, z, t) = 2\pi \int_0^\infty dk k^2 \int_0^\pi d\theta \sin\theta A(k, \theta) J_0 \\ \times (k\rho \sin\theta) \exp[ik(z \cos\theta - ct)], \quad (3) \end{aligned}$$

where $A(k, \theta)$ is the cylindrically symmetric Whittaker-type angular spectrum of plane waves, $J_0(k\rho \sin \theta)$ denotes zeroth-order Bessel function of the first kind, θ and $k = \omega/c$ are the cone angle and carrier wave number of the Bessel beam, respectively. It can be demonstrated [17], that the instantaneous intensity distribution of such a superposition propagates without any spread, if only the on-axis group velocity of the monochromatic Bessel beams $v_g = (dk_z/d\omega)^{-1}$, where $k_z = k \cos \theta$, is constant over the spectral range of the wave field. The corresponding angular spectrum can be expressed by means of Dirac δ function as

$$A(k, \theta) = \tilde{A}(k) \delta(\theta - \theta_{FWM}(k)). \quad (4)$$

The essential part of this expression is the function $\theta_{FWM}(k)$ determining the support of the angular spectrum of the plane wave constituents of the pulse, i.e., the volume of nonzero angular spectrum of plane waves in k space. To provide the nonspreading propagation, the function has to have the form

$$\theta_{FWM}(k) = \arccos \left[\frac{\gamma(k - 2\beta)}{k} \right], \quad (5)$$

where constant γ determines the group velocity of the wave field as $v_g = c/\gamma$ and parameter 2β has an interpretation as being the wave number of the plane wave component of the angular spectrum that propagates perpendicularly to z axis [see Fig. 1(a) for some examples of the supports of angular spectrum for different parameters γ and β]. The function $\tilde{A}(k)$ in Eq. (4) is the frequency spectrum of the wave field, its exact form defines the spatial shape of the wave field.

The angular spectrum of plane waves (4) with Eq. (5) gives the general solution (3) the following form:

$$\begin{aligned} \Psi_{FWM}(\rho, z, t) = & 2\pi \exp[-i2\gamma\beta z] \int_0^\infty dk k^2 \\ & \times \sin[\theta_{FWM}(k)] \tilde{A}(k) \\ & \times J_0(k\rho \sin \theta_{FWM}(k)) \exp[ik(\gamma z - ct)], \end{aligned} \quad (6)$$

or

$$\begin{aligned} \Psi_{FWM}(\rho, z, t) = & \exp[-i2\gamma\beta z] \int_0^\infty dk A(k) \\ & \times J_0(k\rho \sin \theta_{FWM}(k)) \exp[ik(\gamma z - ct)], \end{aligned} \quad (7)$$

where we have denoted

$$A(k) = 2\pi k^2 \tilde{A}(k) \sin[\theta_{FWM}(k)]. \quad (8)$$

In what follows the Eq. (7) is referred to as a definition of FWM's. The referenced approach [17] implies, that the instantaneous intensity distribution of all the wave fields, expressible as Eq. (7), propagate without any longitudinal or transversal spread, the support of angular spectrum of plane waves (5) being the necessary and sufficient condition for

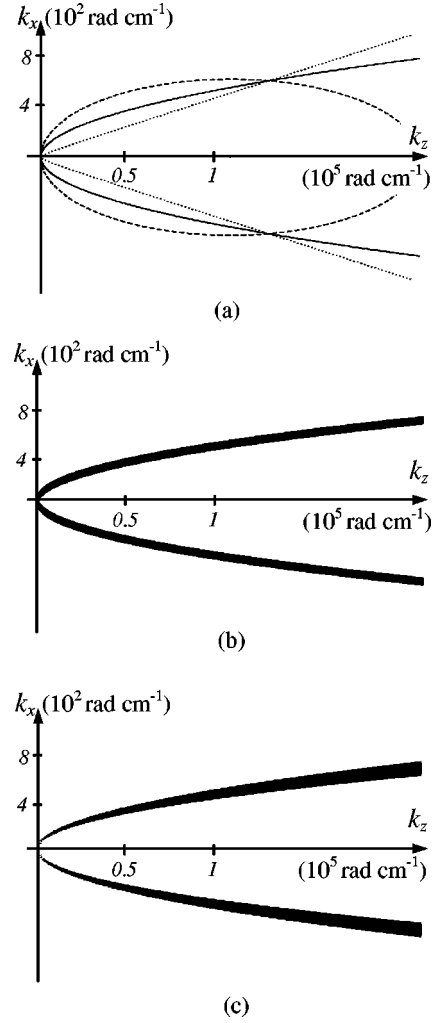


FIG. 1. Supports of angular spectra of plane waves of various LW's: (a) Fundamental LW's (FWM) of different group velocity $v_g = c$ ($\gamma = 1$ and $\beta = 0.4 \text{ rad/cm}^{-1}$) [see Eqs. (4) and (5)], for dashed line $v_g < c$ ($\gamma = 1.000\ 01$ and $\beta = 1 \text{ rad/cm}^{-1}$), for dotted line $v_g > c$ ($\gamma = 0.999\ 994$ and $\beta = 0.4 \text{ rad/cm}^{-1}$); (b) A typical support of angular spectrum of plane waves of finite energy flow LW's, derived in this paper ($\gamma = 1$, $\beta = 0.4 \text{ rad/cm}^{-1}$); (c) A typical support of angular spectrum of plane waves of the finite energy flow LW's derived as superposition of FWM's ($\gamma = 1$, $\beta \sim 0.4 \text{ rad/cm}^{-1}$).

such a behavior. Generally, the spatial amplitude distribution of the FWM's is not propagation invariant, as can be seen from the term $\exp[-i2\gamma\beta z]$ in Eq. (7).

The more conventional definition for the FWM's in Eq. (1) can be shown to be a special case of the definition (7) [17]. Also, it has been shown [17] that in all practical cases the representation (7) does not include any backward propagating plane wave components.

III. A PRACTICAL APPROACH TO OPTICALLY REALIZABLE LW'S

As was already mentioned, one of the main reasons for introducing various LW's has been the need for finite energy flow, i.e., physically realizable approximation to FWM's.

The following discussion is also set up as a derivation of such an approximation. However, being a straightforward application of fundamental principles of Fourier optics, our approach can also be easily implemented by means of a realistic optical setup.

Let us start by mentioning a fundamental property of FWM's, not given sufficient attention in this context so far: as can be seen from the Eqs. (4) and (7), a FWM can be represented as a specific superposition of monochromatic Bessel beams

$$\Psi_B(\rho, z, t; k) = J_0(k\rho \sin \theta_{FWM}(k)) \times \exp\{ik[z \cos \theta_{FWM}(k) - ct]\} \quad (9)$$

of different cone angles θ and carrier wave numbers k , the parameters being connected by the relation (5) [see Fig. 1(a)]. Of course, considering monochromatic components of wideband wave fields instead of the entire superposition is a common method to simplify the study of complex wave fields. In our case, however, the advantage is even more substantial—as far as the frequency spectrum $A(k)$ in Eq. (7) is square integrable, the infinite energy flow of the FWM's in Eq. (7) is a direct consequence of the infinite energy content of its monochromatic components—Bessel beams (9) [2], i.e., the representation does not eliminate the main subject of our discussion. Instead, it suggests a straightforward idea for an approach to finite energy flow approximations to FWM: one has to find a finite energy flow approximation to monochromatic Bessel beams, substitute the result into Eq. (7) and verify that the resulting superposition still represents a wave field that propagates as a LW.

The properties and optical generation of monochromatic Bessel beams have been investigated in great detail during the last decade (see, e.g., Refs. [2,18,19], and references therein). One of their properties, verified both theoretically and experimentally, is particularly useful in our discussion. Namely, it has been shown, that applying finite aperture to a Bessel beam provides us with a finite energy flow wave field, that is a very good approximation of the infinite-aperture Bessel beams (9) in a certain finite depth, near axis volume [2,18,19]. Also, it has been shown experimentally, that the spatial amplitude distributions of the polychromatic superpositions of those apertured Bessel beams approximate very closely the spatial amplitude distributions of the superpositions of “nonapertured” Bessel beams in this volume [20–22]. Such a behavior can be easily explained in terms of angular spectrum representation of scalar wave fields. In this picture a monochromatic Bessel beam is a cylindrically symmetric superposition of plane waves that propagate at angle θ relative to z axis [2]. As the apertured plane waves approximate the amplitude distribution of their infinite aperture counterparts very closely in their central parts (see Fig. 2), one can also observe a very good approximation to the infinite-aperture Bessel beam in this near-axis volume (see Ref. [19] for more detailed description). If the cone angle of a Bessel beam is small, as is always the case in paraxial optical systems, the apertured Bessel beam would behave as its infinite-aperture counterpart (9) for several meters of propagation [2].

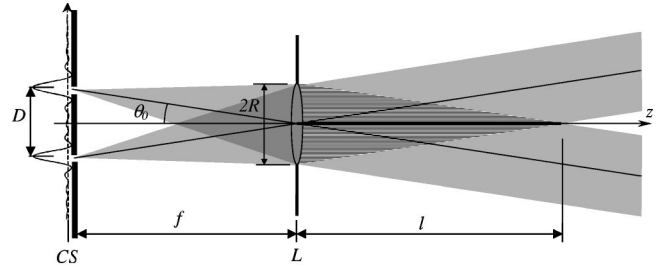


FIG. 2. On the propagation length and angular spectrum of plane waves of apertured Bessel beams. In the simplest case the apertured, finite energy flow approximations to Bessel beams can be generated by means of a circular slit (CS) of diameter D and a lens (L) of focal length f . The propagation length l of the near-axis part of such a beam (the striped region on the figure) is determined as $R/\tan \theta$ where R is the radius of the lens and $\theta = \arctan(D/2f)$ is the cone angle of the Bessel beam. In the front focal plane of the lens the Weyl-type angular spectrum of plane waves of an apertured Bessel beam is sketched.

Thus, the substitution of infinite-aperture Bessel beams in Eq. (7) by their apertured counterparts should generate a finite energy flow wave field, the spatial amplitude distribution of which is a good approximation of the FWM (7) in some finite volume, determined by the simple geometrical construction, shown in Fig. 2.

To derive the mathematical expression for such a wave field, we have to calculate the angular spectrum of plane waves of an apertured Bessel beam A_{AB} . This can be done by calculating the two-dimensional Fourier transform of the transversal amplitude distribution $t(\rho)J_0(\chi_0\rho)$ of the wave field, $t(\rho)$ being the complex-amplitude transmission function of the aperture and $\chi = k \sin \theta$ being the k_{xy} plane projection of the wave vector. Given the Weyl-type angular spectrum of plane waves of the infinite-aperture Bessel beam

$$A_B(\chi) = \tilde{A} \delta(\chi - \chi_0), \quad (10)$$

where \tilde{A} is a constant, the Fourier transform can be found to yield

$$\begin{aligned} A_{AB}(\chi) &= \frac{\tilde{A}}{(2\pi)^2} T(\chi) * \delta(\chi - \chi_0) \\ &= \frac{\chi_0 \tilde{A}}{(2\pi)^2} \int_0^{2\pi} d\varphi T(\sqrt{\chi^2 + \chi_0^2 - 2\chi\chi_0 \cos(\varphi - \varphi_0)}), \end{aligned} \quad (11)$$

where $T(\chi)$ is the two-dimensional Fourier transform of the transmission function and $*$ denotes the convolution operation (see also Ref. [23]). The argument $\sqrt{\chi^2 + \chi_0^2 - 2\chi\chi_0 \cos(\varphi - \varphi_0)}$ has an interpretation as being the distance between the points (χ, φ) and (χ_0, φ_0) , φ being the polar angle of k_{xy} plane. As for all convenient apertures, the function $T(\chi)$ is well localized around zero, the major contribution to the integral (11) obviously comes from small values of φ and one can write in good approximation

$$A_{AB}(\chi) \approx \frac{\chi_0 \tilde{A}}{2\pi} T(\chi - \chi_0). \quad (12)$$

The interpretation of the expression (12) is straightforward: the finite aperture gives the support of angular spectrum of a monochromatic Bessel beam a finite “width” (see Fig. 2 for an illustrative example). Exact form of the support is determined by the complex-amplitude transmission function, however, the well-known set of fundamental Fourier transform pairs gives a good idea of what the support of angular spectrum looks like, without any calculations.

Obviously the finite aperture has a similar effect on the angular spectrum support of a FWM—the δ function in Eq. (4) is substituted by a weighting function and the angular spectrum of plane waves of apertured FWM’s can be written as

$$\begin{aligned} A_{AFWM}(k, \chi) &= \frac{\chi_{FWM}(k) \tilde{A}(k)}{(2\pi)^2} \int_0^{2\pi} d\varphi \\ &\quad \times T(\sqrt{\chi^2 + \chi_{FWM}(k)^2 - 2\chi\chi_{FWM}(k)\cos\varphi}) \\ &\approx \frac{\chi_{FWM}(k) \tilde{A}(k)}{2\pi} T(\chi - \chi_{FWM}(k)), \end{aligned} \quad (13)$$

where $\chi_{FWM}(k) = k \sin \theta_{FWM}(k)$ or

$$\begin{aligned} A_{AFWM}(k, \chi) &= A(k) \int_0^{2\pi} d\varphi \\ &\quad \times T(\sqrt{\chi^2 + \chi_{FWM}(k)^2 - 2\chi\chi_{FWM}(k)\cos\varphi}), \end{aligned} \quad (14)$$

where we have denoted

$$A(k) = \frac{\chi_{FWM}(k) \tilde{A}(k)}{2\pi}. \quad (15)$$

Consequently, the Weyl-type plane wave expansion of the wave field behind the aperture can be written as

$$\begin{aligned} \Psi_{AFWM}(\rho, z, t) &= 2\pi \int_0^\infty dk \int_0^\infty d\chi \chi A_{AFWM}(k, \chi) \\ &\quad \times J_0(\rho\chi) \exp\left[ik \left(z \sqrt{1 - \left(\frac{\chi}{k}\right)^2} - ct \right). \right] \end{aligned} \quad (16)$$

Alternatively, the transformation $\chi = k \sin \theta$ gives the expression (16) the following form:

$$\begin{aligned} \Psi_{AFWM}(\rho, z, t) &= 2\pi \int_0^\infty dk k^2 \int_0^{2\pi} d\theta \sin \theta \cos \theta \\ &\quad \times A_{AFWM}(k, k \sin \theta) J_0(k\rho \sin \theta) \\ &\quad \times \exp[ik(z \cos \theta - ct)]. \end{aligned} \quad (17)$$

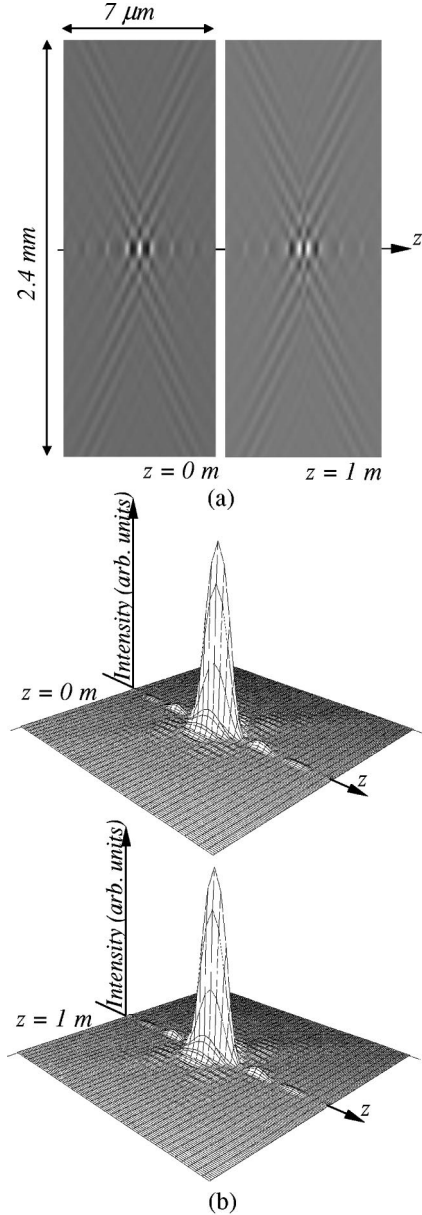


FIG. 3. The results of a numerical evaluation of propagation of apertured FWM in Eq. (23). (a) A gray-scale plot of the spatial amplitude distribution of the apertured FWM in the xz plane at distances $z=0$ m and $z=1$ m; (b) Instantaneous intensity distribution of the wave field in the xz plane in those positions.

An example of an apertured FWM (17) is depicted in Fig. 3. One can see, that the wave field still has the characteristic narrow central peak. In fact, the spatial amplitude distributions of apertured and nonapertured FWM’s do not differ noticeably in the near-axis volume except for the finite propagation length of apertured FWM’s (we present some numerical results on their propagation in the following section). The support of the angular spectrum of plane waves (14) of the derived wave field is depicted in Fig. 1(b)—as compared with the supports of angular spectrum of a nonapertured FWM’s [see Fig. 1(a)] the former has a finite “thickness.”

The wave field (16) is derived by applying a finite aperture to a FWM (7). However such a method does not offer a means of optical generation of those wave fields *per se*—we still assume a FWM as the initial wave field on the aperture.

To get an optically realizable approach we once more use the properties of apertured Bessel beams, or more specifically, the angular spectrum description of their optical generation (see Fig. 2). Namely, as the apertured FWM's are superpositions of apertured Bessel beams and the latter can be formed from apertured plane waves (or spherical waves), one can generate the entire spectrum of the monochromatic components by illuminating a Bessel beam generator (axicon, circular diffraction grating) by a polychromatic, apertured plane wave. Still, the optical implementation is far from trivial, as the setup has to be constructed in such a way, that the central cone angles of the apertured Bessel beam components depend on their wave number as $\theta_{FWM}(k)$ (5). However, the experimental implementation of such cone angle dispersion has been addressed in our recent publication [17] where it has been shown, that the wavelength dispersions of cone angle, generated by various Bessel beam generators, can be combined to yield a very good approximation to the angular spectrum of a FWM in an ultrawide bandwidth (corresponding to a 4-fs pulse). Thus, there are no fundamental difficulties in optical generation of the apertured FWM's. Some of the experimental difficulties are mentioned in Sec. V below.

To summarize the preceding discussion, we propose the wave field (17) as a class of finite energy flow LW's. The wave field has the following properties. (i) The energy flow of the wave field is finite if only the applied aperture is finite; (ii) In the limit, as the aperture is extended to infinity, the function T in Eq. (17) converges to δ function and the wave field (17) transforms into the FWM (7); (iii) Despite the finite aperture approximation made, the wave field can be constructed so that its spatial amplitude distribution still has the characteristic micrometer diameter peak and can propagate several meters before the final spread (see the following section for the numerical results); (iv) The wave fields can be generated by means of conventional optical setups.

Also, we can outline the main difference between the LW's, proposed in this paper [Eq. (17)] and LW's, discussed in literature so far [Eq. (2)]. The comparison of their supports of angular spectrum of plane waves in Figs. 1(b) and 1(c) (respectively) shows, that the transversal "width" in k_{xy} plane of angular spectrum of plane waves of our LW's is a constant—such a result is a consequence of applying aperture with a wavelength-independent complex-amplitude transmission function. On the other hand, the transversal width is not constant for the superpositions of FWM's in Eq. (2) and the preceding discussion gives the property a straightforward interpretation: the corresponding aperture has a wavelength-dependent complex-amplitude transmission function. In the context of our discussion, where the main goal is optical realizability, such an approach should be regarded as an impractical one. There is simply no need for implementation of such an aperture.

IV. NUMERICAL RESULTS

As an example we present numerical results for an apertured FWM with the following parameters: we choose $v_g = c$ ($\gamma = 1$) for the group velocity, the constant $\beta = 40 \text{ rad/m}^{-1}$ [$\theta_{FWM}(k) \approx 0.22^\circ$ for 600 nm], the fre-

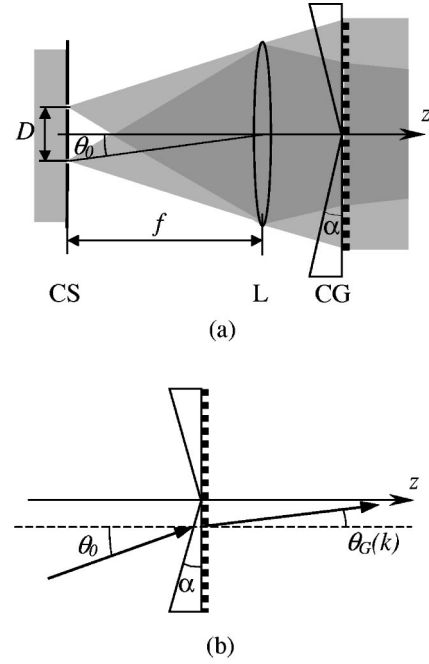


FIG. 4. Optical generation of apertured FWM's. (a) Optical setup consists of a circular slit (SC) of diameter D , a lens (L) of focal length f , and of a circular grating (CG) (see text); (b) On sign conventions in Eq. (18).

quency spectrum $A(k)$ is rectangular and has a bandwidth of a 4-fs pulse (400 nm–800 nm) [see Fig. 3(a) for the spatial amplitude distribution and Fig. 1(b) for the support of angular spectrum of such a wave field].

The optical setup, that generates the angular dispersion of cone angles of the apertured FWM is depicted in Fig. 4(a) [17]. The optical scheme consists of a circular slit, a lens (L), and a circular diffraction grating on the surface of an axicon, so-called circular grism. The circular slit is illuminated with a wideband plane wave pulse (with a specific phase distortion, if necessary) and the lens forms a polychromatic superposition of apertured Bessel beams (so-called Bessel-X pulse [15,21]). The task of the circular grism is to introduce the FWM-specific angular dispersion into the support of the angular spectrum of the wave field. It can be shown [17], that given the cone angle of the apertured Bessel beams behind the lens $\theta_0 = \arctan(D/2f)$ [D is the diameter of the circular slit and f is the focal length of the lens, see Fig. 4(a)] the wavelength-dependent cone angle of the Bessel beam components of the resulting wave field can be expressed as

$$\theta_G(k) = \arcsin \left\{ \frac{2\pi}{kd} + n(k) \times \sin \left[-\alpha + \arcsin \left(\frac{1}{n(k)} \sin(\theta_0 + \alpha) \right) \right] \right\}, \quad (18)$$

where d is the grating constant, α is the axicon angle, and $n(k)$ is the refractive index of the axicon material [sign conventions are chosen so that the angles α , θ_0 , $\theta_G(k)$ are positive in Fig. 4(b)]. The function $\theta_G(k)$ can be optimized so the relation $\theta_G(k) = \theta_{FWM}(k)$ is satisfied for a set of three

wavelengths (400 nm, 600 nm, 800 nm) yielding for the parameters θ_0 , α , d the following values:

$$\begin{aligned}\theta_0 &= 9.4683 \times 10^{-3} \text{ rad}, \\ \alpha &= 1.3866 \times 10^{-2} \text{ rad}, \\ d &= 3.7509 \times 10^{-4} \text{ m}.\end{aligned}\quad (19)$$

By applying this result on the Eq. (14) one finds, that the angular spectrum of the wave field behind the composite optical element (see Fig. 4) can be described by the equation,

$$\begin{aligned}A_{AFWM}(k, \chi) &= A(k) \int_0^{2\pi} d\varphi \\ &\times T(\sqrt{\chi^2 + \chi_G(k)^2 - 2\chi\chi_G(k)\cos\varphi}),\end{aligned}\quad (20)$$

where $\chi_G(k) = k \sin[\theta_G(k)]$. For the sake of simplicity let us choose the aperture to be circular with radius R . The Fourier transform of the transmission function in this case can be found to be

$$T(\chi) = \frac{2\pi R}{\chi} J_1(R\chi) \quad (21)$$

and the corresponding angular spectrum of plane waves reads

$$\begin{aligned}A_{AFWM}(k, \chi) &= \tilde{A}(k) \frac{\chi_G(k)R}{2\pi} \int_0^{2\pi} d\varphi \\ &\times \frac{J_1(R\sqrt{\chi^2 + \chi_G(k)^2 - 2\chi\chi_G(k)\cos\varphi})}{\sqrt{\chi^2 + \chi_G(k)^2 - 2\chi\chi_G(k)\cos\varphi}}.\end{aligned}\quad (22)$$

Thus, the spatial amplitude distribution of the corresponding apertured FWM can be described by [see Eq. (16)]

$$\begin{aligned}\Psi_{AFWM}(\rho, z, t) &= 2\pi \int_0^\infty dk \int_0^\infty d\chi \chi A_{AFWM}(k, \chi) \\ &\times J_0(\rho\chi) \exp\left[ik\left(z\sqrt{1 - \left(\frac{\chi}{k}\right)^2} - ct\right)\right],\end{aligned}\quad (23)$$

where $A_{AFWM}(k, \chi)$ is described by Eq. (22).

The results of a numerical evaluation of Eq. (23) for 2 cm aperture ($R = 1$ cm) under the assumption of a real frequency spectrum $A(k)$ are depicted in Fig. 3. In Fig. 3(a) the wave field is in its initial position ($z = 0$, $t = 0$), in Fig. 3(b) the wave field has propagated to position $z = 1$ m. First of all, one can see, that the apertured, i.e., optically realizable FWM's preserve the most significant property of the FWM's (7)—the narrow central peak of the spatial amplitude distribution. In fact, the FWM and corresponding apertured FWM (23) have practically identical spatial amplitude distributions in the near-axis volume, depicted in Fig. 2. As for propaga-

tion, the comparison of Figs. 3(a) and 3(b) shows that the instantaneous spatial intensity distribution for such a setup propagates up to 1 m without any spread.

The wave field (23) could also be calculated by means of Fresnel diffraction integrals. In this case the wave field behind the circular grism should be expressed as

$$\begin{aligned}\Psi_{AFWM}(\rho, z, t) &= \frac{c}{i\lambda z} \int_0^\infty dk A(k) \exp[ikct] \int_0^R d\rho\rho \\ &\times J_0(k\rho \sin\theta_G(k)) \\ &\times J_0\left(\frac{k\rho\rho'}{z}\right) \exp\left[ik\left(\frac{\rho'^2 + \rho^2}{2z}\right)\right]\end{aligned}\quad (24)$$

(see Ref. [17] for related discussion). However we will not resolve this (quite complex) expression, as the Fresnel integrals of this type have already been investigated extensively by means of the method of stationary phase (see, for example, Refs. [17,18,24]). It has been shown, that the integration over the radial distance ρ yields a monochromatic Bessel beam of the cone angle $\theta_{FWM}(k)$, the propagation distance of which can be estimated by the construction, depicted in Fig. 2. Thus, the integral (24) in this approximation yields a superposition of Bessel beams similar to the integral representation of FWM in Eq. (7).

V. EXPERIMENTAL CONSIDERATIONS

Though there is really no fundamental problem with the realization of the proposed setup, one has to tackle several technical obstacles. First of all, to generate a highly localized pulse, as the one depicted in Fig. 3, one has to drive the setup with a 4 fs pulse and the optical wave fields with such a bandwidth are highly susceptible to phase distortions, introduced by dispersive media. Even though a FWM propagates without any lateral and longitudinal spread irrespective of the exact form of its (generally complex) frequency spectrum $A(k)$ to get a transform-limited central peak, the relative phases between the Bessel beam constituents of the FWM must vanish. Hence, one has to apply conjugated phase distortion to the input pulse to compensate for various phase distortions in the setup. Also, the dispersive properties of the air have to be taken into account.

The second difficulty worth mentioning here is the relative complexity of producing the introduced optical element—circular grism. Namely, it may be surprising but the fabrication and polishing of a high-quality, concave conical surface is still a complicated task. Also, the blazed diffraction grating has to be fabricated on the circular grism so as to eliminate the higher order diffraction.

VI. CONCLUSIONS

In this paper we gave a physically transparent approach to construction of realizable, finite energy flow LW solutions of the scalar homogeneous wave equation. By means of well-

known properties of apertured Bessel beams we demonstrated that an optically realizable, finite energy flow set of LW's can be obtained by applying finite aperture to fundamental LW's—FWM's. We derived a convenient integral representation for those wave fields and proposed a conventional optical setup for their optical generation. The presented numerical simulations show, that the optical setup

generates LW's with very narrow beam waist that propagate over reasonable distances.

ACKNOWLEDGMENT

This research was supported by the Estonian Science Foundation Grant No. 3866.

-
- [1] J.N. Brittingham, *J. Appl. Phys.* **54**, 1179 (1983).
 - [2] J. Durnin, J.J. Miceli, Jr., and J.H. Eberly, *Phys. Rev. Lett.* **58**, 1499 (1987).
 - [3] J. Lu and J.G. Greenleaf, *IEEE Trans. Ultrason. Ferroelectr. Freq. Control* **39**, 19 (1992).
 - [4] J. Fagerholm, A.T. Friberg, J. Huttunen, D.P. Morgan, and M.M. Salomaa, *Phys. Rev. E* **54**, 4347 (1996).
 - [5] R.W. Ziolkowski, *J. Math. Phys.* **26**, 861 (1985).
 - [6] R.W. Ziolkowski, *Phys. Rev. A* **39**, 2005 (1989).
 - [7] I. Besieris, M. Abdel-Rahman, A. Shaarawi, and A. Chatzipetros, *Prog. Electromagn. Res.* **19**, 1 (1998).
 - [8] R.W. Ziolkowski, I.M. Besieris, and A.M. Shaarawi, *J. Opt. Soc. Am. A* **10**, 75 (1993).
 - [9] A.M. Shaarawi, *J. Opt. Soc. Am. A* **14**, 1804 (1997).
 - [10] A.M. Shaarawi, I.M. Besieris, R.W. Ziolkowski, and S.M. Sedky, *J. Opt. Soc. Am. A* **12**, 1954 (1995).
 - [11] P.L. Overfelt, *Phys. Rev. A* **44**, 3941 (1991).
 - [12] A.M. Shaarawi, R.W. Ziolkowski, and I.M. Besieris, *J. Math. Phys.* **36**, 5565 (1995).
 - [13] R. Donnelly and R.W. Ziolkowski, *Proc. R. Soc. London, Ser. A* **440**, 541 (1993).
 - [14] R. Donnelly and R.W. Ziolkowski, *Proc. R. Soc. London, Ser. A* **437**, 673 (1992).
 - [15] P. Saari and H. Sõnajalg, *Laser Phys.* **7**, 32 (1997).
 - [16] P. Saari, in *Proceedings of the International Conference, Naples, 2000*, edited by D. Mugnai, A. Ranfagni, and L. S. Schulman (Italian CNR, Roma, 2001), p. 37.
 - [17] K. Reivelt and P. Saari, *J. Opt. Soc. Am. A* **17**, 1785 (2000).
 - [18] A. Vasara, J. Turunen, and A.T. Friberg, *J. Opt. Soc. Am. A* **6**, 1748 (1989).
 - [19] R. Borghi, S. Santarsiero, and F. Gori, *J. Opt. Soc. Am. A* **14**, 23 (1997).
 - [20] H. Sõnajalg, M. Rätsep, and P. Saari, *Opt. Lett.* **22**, 310 (1997).
 - [21] P. Saari and K. Reivelt, *Phys. Rev. Lett.* **79**, 4135 (1997).
 - [22] S. Chavez-Cerda *et al.*, *Opt. Express* **3**, 524 (1998).
 - [23] Z. Bouchal, *J. Mod. Opt.* **40**, 1325 (1993).
 - [24] H. Sõnajalg and P. Saari, *Opt. Lett.* **21**, 1162 (1996).